ISET Journal of Earthquake Technology, Paper No. 491, Vol. 44, No. 3-4, Sept.-Dec. 2007, pp. 391–408

MITIGATION OF SEISMIC FINANCIAL RISK OF REINFORCED CONCRETE WALLS BY USING DAMAGE AVOIDANCE DESIGN

R.K. Khare*, R.P. Dhakal**, J.B. Mander***, N.B.A. Hamid**** and M.M. Maniyar*

*Department of Civil Engineering, S.G.S. Institute of Technology & Science, Indore-452003
**Department of Civil Engineering, University of Canterbury, Private Bag 4800, Christchurch, New Zealand
***Zachry Department of Civil Engineering, Texas A&M University, College Station, Texas, U.S.A.
****Faculty of Civil Engineering, University Teknologi Mara, Shah Alam, Selangor, Malaysia

ABSTRACT

Seismic financial risk analyses of rocking precast prestressed reinforced concrete hollow-core walls designed using the Damage Avoidance Design (DAD) philosophy and of code-compliant ductile monolithic walls are performed based on the results of experimental investigation on the seismic behaviour of wall specimens representing the two different systems. Incremental dynamic analyses (IDA) are performed on nonlinear computational models of the two prototype walls, and experimental results are used to calibrate different damage states. Fragility curves are then developed for the two wall systems and the expected annual loss (EAL) is calculated based on a probabilistic financial risk assessment framework. The structural performance and financial implications of the two wall systems are compared. The study shows that it is the structurally acceptable minor-to-moderate damage that is responsible for a major share of the financial risk. Damage avoidance philosophy avoids this minor–moderate damage and hence reduces the financial risk greatly.

KEYWORDS: Walls, Seismic Risk, Expected Annual Loss (EAL), Damage Avoidance Design (DAD), Incremental Dynamic Analysis (IDA)

INTRODUCTION

For constructed facilities seismic risk will be understood better by all stakeholders if it is expressed in monetary terms rather than in terms of technical parameters representing performance measures. As performance-based earthquake engineering (PBEE) aims to satisfy the diverse needs of the society, it should ensure that the performance of designed structures is adequate not only in terms of safety and damage but also in terms of financial risk. In Earthquake Engineering the innovation and use of probabilistic financial risk assessment methodologies have been increasing over the last two decades. Pacific Earthquake Engineering Research (PEER) Center has developed a probabilistic seismic risk assessment framework in the form of a triple integral equation (Krawinkler and Miranda, 2004) which can be used to approximate the probability of a decision criterion being satisfied. The final decision variable in the current PEER triple integral formulation can represent the probability of exceeding a performance requirement, which can be set to any level. Dhakal and Mander (2006) extended the PEER triple integral to give an additional dimension—time, which allows the integration of all probable losses over time to obtain a dollar value that would indicate the annual financial risk of the structure/system due to all possible seismic hazards. This is certainly a more useful interpretation of seismic risk, which is easily understood by the non-engineering community and all stakeholders of a structure.

The current seismic design philosophy aims to prevent loss of life by avoiding collapse but accepts damage due to moderate-to-large earthquakes for the type of structures under consideration. Nevertheless, financial risk assessment methodologies suggest that the repair of the so-called acceptable minor-moderate damage contributes a significant proportion to the seismic financial risk. Therefore, more focus is being given recently to avoid these repairable damages during moderate earthquakes. Damage Avoidance Design (DAD) philosophy is one approach whereby higher performance objectives at different levels of earthquakes can be achieved without causing any structural damage to the constructed facilities. Such a conceptual design approach was proposed by Mander and Cheng (1997) for bridge substructures, whereby rocking columns form the seismic resistance mechanism. Since then several experimental investigations have been carried out to compare seismic performance of reinforced concrete (RC) rocking bridge piers and moment resisting frames designed according to the conventional ductile design approach

and to the emerging damage avoidance concept (Michael, 2003; Arnold, 2004; Li, 2006; Mashiko, 2006). The experimental results have also been extended to develop fragility curves and then to assess seismic financial risk of RC bridges (Dhakal and Mander, 2006).

Seismic performance of conventional reinforced concrete walls and unbonded post-tensioned precast concrete walls has been experimentally investigated by several researchers (Holden et al., 2003; Ajrab et al., 2004; Kurama et al., 1997, 2002). Furthermore, seismic design of unbonded post-tensioned precast concrete walls has also been studied extensively (Kurama, 2000, 2005; Perez et al., 2004; Bora et al., 2007). Nevertheless, the authors are not aware either of any study on seismic financial risk assessment of any kind of reinforced concrete walls or of a detailed comparison between the seismic performances of a fixed-end monolithic wall designed for ductility and a precast rocking wall designed for damage avoidance. This paper first explains a quadruple integral formula to assess seismic financial risk of engineering systems and then uses this framework to assess and compare the financial risks of two wall systems designed for ductility and damage avoidance. This paper also summarises the experimental investigations on the seismic performance of monolithic ductile walls and precast rocking walls, based on which the damage models for these two wall designs are established. Thus, established damage models are combined with nonlinear incremental dynamic analysis (IDA) results, seismic hazard-recurrence relationship, and logically established loss models to estimate the probable financial loss for the two wall systems.

OVERVIEW OF THE PROCESS

1. Financial Seismic Risk Assessment Framework

Communicating seismic vulnerability to decision makers is an important aspect of performance-based earthquake engineering (PBEE). One such communication tool is expected annual loss (EAL), which can be expressed in a dollar value. It incorporates the entire range of seismic scenarios, return rates, and expected damages into a median dollar loss. Though there are many methods of quantifying financial risk, EAL is especially useful to decision makers for the cost-benefit analysis of various design alternatives for new structures or of various seismic retrofit alternatives for existing structures. Moreover, EAL can easily be accounted for via inclusion into the operating budgets.

Recent research at Pacific Earthquake Engineering Research (PEER) Center on seismic risk assessment has led to a mathematical expression in the form of a triple integral (Krawinkler and Miranda, 2004) that can be used to evaluate the probability of a chosen decision variable exceeding a prescribed limit. The interrelationships used in the triple integration link firstly seismic hazard to structural response, then response to damage, and finally damage to the decision variable. If the decision variable is expressed in terms of the economic consequences, the triple integral expression can be used to estimate the total probable loss due to an earthquake. Dhakal and Mander (2006) have extended the PEER framework formula to a quadruple integral by including time, thereby enabling the quantification of seismic risk in terms of EAL. The quadruple integral formulation is given as

$$\mathrm{EAL} = \int\int\int\int L_R \left|\mathrm{d}P\left[L_R \mid \mathrm{DM}\right]\right|\left|\mathrm{d}P\left[\mathrm{DM} \mid \mathrm{EDP}\right]\right|\left|\mathrm{d}P\left[\mathrm{EDP} \mid \mathrm{IM}\right]\right|\left|\mathrm{d}f_a\left[\mathrm{IM}\right]\right| \tag{1}$$

in which, IM = intensity measure; f_a [IM] = annual probability of an earthquake of a given intensity IM; EDP = engineering demand parameter; DM = damage measure; L_R = loss ratio (i.e., decision variable); $P[A \mid B]$ = shortened form of the conditional probability $P[A \geq a \mid B = b]$; and $\mathrm{d}P[A \mid B]$ = derivative of $P[A \mid B]$ with respect to A. It may be noted that although Equation (1) can be applied with minor modifications (if needed) to account for the loss due to drift-related non-structural damage and acceleration-related content damage, the application in this paper is strictly confined to the estimation of probable loss due to the damage of structural and non-structural walls only. Needless to mention, the implications of downtime and death are not incorporated.

It is apparent that to calculate EAL using Equation (1), interrelationships between f_a and IM, IM and EDP, EDP and DM, and DM and L_R are needed. Equation (1) can be converted to a closed form equation and the calculation of EAL can be performed manually if all the abovementioned interrelationships are expressed in simple algebraic forms. Nevertheless, the integration processes have to be performed numerically if simple algebraic expressions do not exist for any of the aforementioned interrelationships.

In this paper, the integration process is performed numerically for the reinforced concrete walls that are typically used in warehouse type buildings. Although this study concentrates on the behaviour of walls, the results also shed light on the behaviour of such single-storey industrial buildings as side-walls are the major and dominating component of these buildings. In moment-resisting frame buildings though, a wall is just one of the several components whether it is structural (in the case of shear walls) or non-structural (in the case of partition walls). It may be noted that the precast walls designed to rock only at the base (as studied in this paper) fairly represent both structural and non-structural rocking walls. Such walls, if used for partitioning (as non-structural component), will need a rocking connection only at the base. Similarly, rocking shear walls (as structural component) usually span to the top of the building without being disturbed by a frame in between; hence a rocking connection at the base only is sufficient.

2. Target Structure

Precast concrete wall panels are commonly used as primary lateral load resisting system for the construction of warehouses, shopping complexes, residential houses, commercial buildings, community halls and gymnasiums. Precast wall panels are designed to undergo non-linear response under strong earthquakes, which may result in heavy damage. Use of prestressed tendons, energy dissipaters and steel armouring at the base can help the walls sustain large lateral deformations through rocking and thus avoid the damage. In prestressed wall systems, the tendons, if left unbonded over a certain length, remain elastic during rocking. In this way, the elastic restoring force will essentially prevent residual lateral displacements from occurring. Since the concrete is not bonded to the tendons, considerably less cracking is induced than in the monolithic walls that rely solely on bonded reinforcement to provide the lateral force resistance. The behaviour of such a rocking system can be described by bilinear elastic load-displacement envelope. In such a system, cosmetic damage is restricted to the bottom corners of the wall about which it rocks. By armouring the ends of a prestressed concrete wall with steel plates and by embedding a mating steel plate in the foundation, it is possible to avoid any damage. This introduces the notion of the damage avoidance design (DAD) philosophy, first proposed by Mander and Cheng (1997). One potential disadvantage of this purely bilinear elastic system is the lack of energy dissipation capacity. By externally attaching low-yield-strength-steel fuse bars to the wall unit and to the foundation, a level of hysteretic damping can be introduced to reduce the structure's response to the seismic excitation, while maintaining the self-centering characteristics of the rocking system.

In this paper, seismic risks of a ductile wall with a fixed-end monolithic connection (hereafter referred to as ductile wall) and a rocking precast prestressed wall designed using DAD philosophy (hereafter referred to as DAD wall) are compared. There can be two different grounds for the comparison: either we compare a ductile wall and a DAD wall having the same period, without caring about the design force; or we compare the two walls designed for the same seismic force although the periods might be different. The latter appears to be a more rational approach and hence has been chosen here. The DAD wall and the ductile wall thus considered in this study are shown in Figure 1(a). Both walls are 8 m high, 20 cm thick and 1.2 m long. The precast DAD wall has a hollow-core section whereas the ductile wall has a solid rectangular cross-section. The DAD wall is designed and constructed to ensure that the wall does not crush between the cores due to the concentration of stress coming from the prestressing force and that the mild steel energy dissipaters are perfectly anchored with the wall. Other design and construction details of the DAD wall are given elsewhere (Hamid, 2006). Major design parameters of these two walls are listed in the table in Figure 1(b). For the two different wall designs, the generation of interrelationships between the different parameters involved in the EAL assessment process and the successive numerical integrations are explained below in detail.

IM VERSUS EDP RELATIONSHIP

1. Incremental Dynamic Analysis

Incremental Dynamic Analysis (IDA) procedure developed by Vamvatsikos and Cornell (2002) is adopted here for the analysis of the two walls. IDA basically consists of performing a series of time-history analyses to arrive at a set of EDPs, obtained by scaling the IM to various intensities over a suite of earthquake records. It is similar (though far superior) to a static pushover analysis in that it encompasses the entire range of likely behavior, from pre-yield to collapse. In order to analyse the seismic performances and damage potentials of the two wall systems through IDA, the 20 earthquake records

listed in Table 1, which were first used by Vamvatsikos and Cornell (2004), are used in this study. Response spectra for the 20 earthquake records scaled to the same IMs of PGA = 1.0*g* and spectral acceleration for 5% damping at 1 s period, i.e., S_a(1 s, 5%) = 1.0*g*, are shown in Figures 2(a) and 2(b), respectively. These figures also show the lognormal coefficient of variation (β_D) of the spectral acceleration at different periods for the two cases. It is apparent in Figure 2(a) that β_D across the spectrum is consistent for periods from 0.5 to 1.6 s if the records are scaled according to PGA. On the other hand, although β_D is zero at the scaled period (i.e., at 1 s), it will have a large and inconsistent variation with respect to period when the records are scaled according to S_a(1 s, 5%) (see Figure 2(b)). As the walls considered in this study have natural periods (T_n) less than 1.6 s, it was considered appropriate to use PGA as the IM, owing nearly to the predictability of the uncertainty associated with the PGA-based IM scaling.

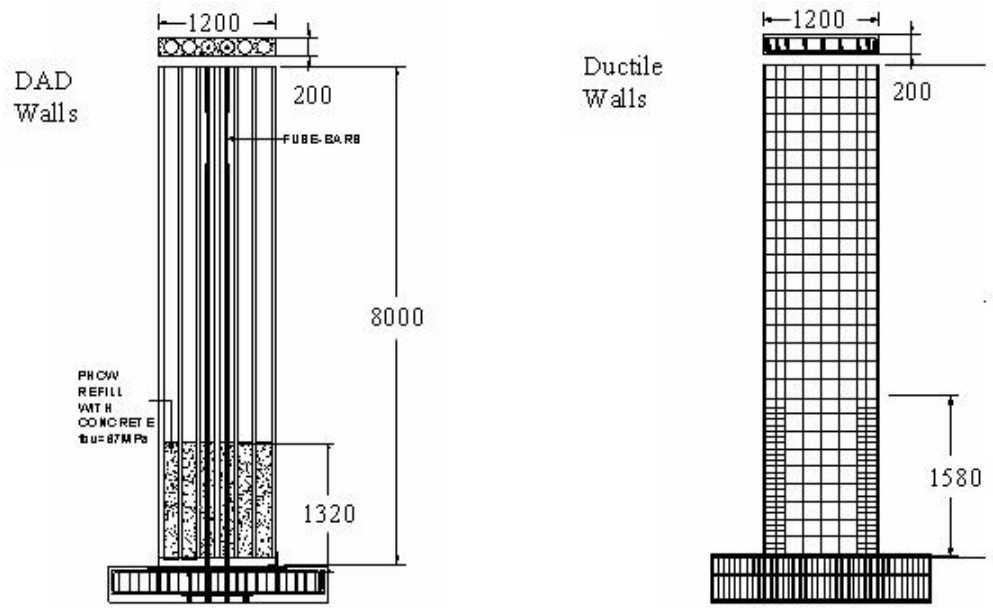

(a)

Parameter	Precast hollow-core	Fixed-end mono-

(b)

Fig. 1 Prototype precast wall panels: (a) models for the dynamic analysis; (b) design parameters

As shown in Figure 3, DAD wall panel is modelled with the "flag-shaped" hysteretic rule, and a modified Takeda rule is adopted to model the performance of the ductile wall panel (Carr, 2003). The two prototype structural walls are idealised by single-degree-of-freedom (SDOF) systems, which are analyzed using a nonlinear structural analysis program RUAUMOKO (Carr, 2003). Geometrical nonlinearity is taken into account in the analyses to include the P-delta effects. Static pushover analysis is conducted before IDA to establish a SDOF model for each type of wall panels. To begin with the IDA, the selected

earthquake records are scaled gradually from a low IM to a high IM, giving an earthquake ground motion that is large enough to cause collapse of the walls. For each increment of IM, a nonlinear dynamic time history analysis is performed. Analyses are continued until structural collapse occurs at a very high IM.

Table 1: Earthquake Ground Motion Records Used in the Study

Label	Event	Year	Station	Φ^* (deg)	M^{**}	R^{***} (km)	PGA (g)
A	Loma Prieta	1989	Agnews State Hospital	90	6.9	28.2	0.159
B	Imperial Valley	1979	Plaster City	135	6.5	31.7	0.057
C	Loma Prieta	1989	Hollister Differential Array	255	6.9	25.8	0.279
D	Loma Prieta	1989	Anderson Dam	270	6.9	21.4	0.244
E	Loma Prieta	1989	Coyote Lake Dam	285	6.5	22.3	0.179
F	Imperial Valley	1979	Cucapah	85	6.9	23.6	0.309
G	Loma Prieta	1989	Sunnyvale Colton Avenue	270	6.6	28.8	0.207
H	Imperial Valley	1979	El Centro Array #13	140	6.5	21.9	0.117
J	Imperial Valley	1979	Westmoreland Fire Station	90	6.5	15.1	0.074
K	Loma Prieta	1989	Hollister South & Pine	0	6.9	28.8	0.371
M	Loma Prieta	1989	Sunnyvale Colton Avenue	360	6.9	28.8	0.209
N	Superstition Hills	1987	Wildlife Liquefaction Array	90	6.7	24.4	0.180
P	Imperial Valley	1979	Chihuahua	282	6.5	28.7	0.254
Q	Imperial Valley	1979	El Centro Array #13	230	6.5	21.9	0.139
R	Imperial Valley	1979	Westmoreland Fire Station	180	6.5	15.1	0.110
S	Loma Prieta	1989	WAHO	0	6.9	16.9	0.370
T	Superstition Hills	1987	Wildlife Liquefaction Array	360	6.7	24.4	0.200
U	Imperial Valley	1979	Plaster City	45	6.5	31.7	0.042
V	Loma Prieta	1989	Hollister Differential Array	165	6.9	25.8	0.269
W	Loma Prieta	1989	WAHO	90	6.9	16.9	0.638

*Component; **Moment magnitude; ***Closest distance to fault rupture (source: PEER Strong Motion Database[1])

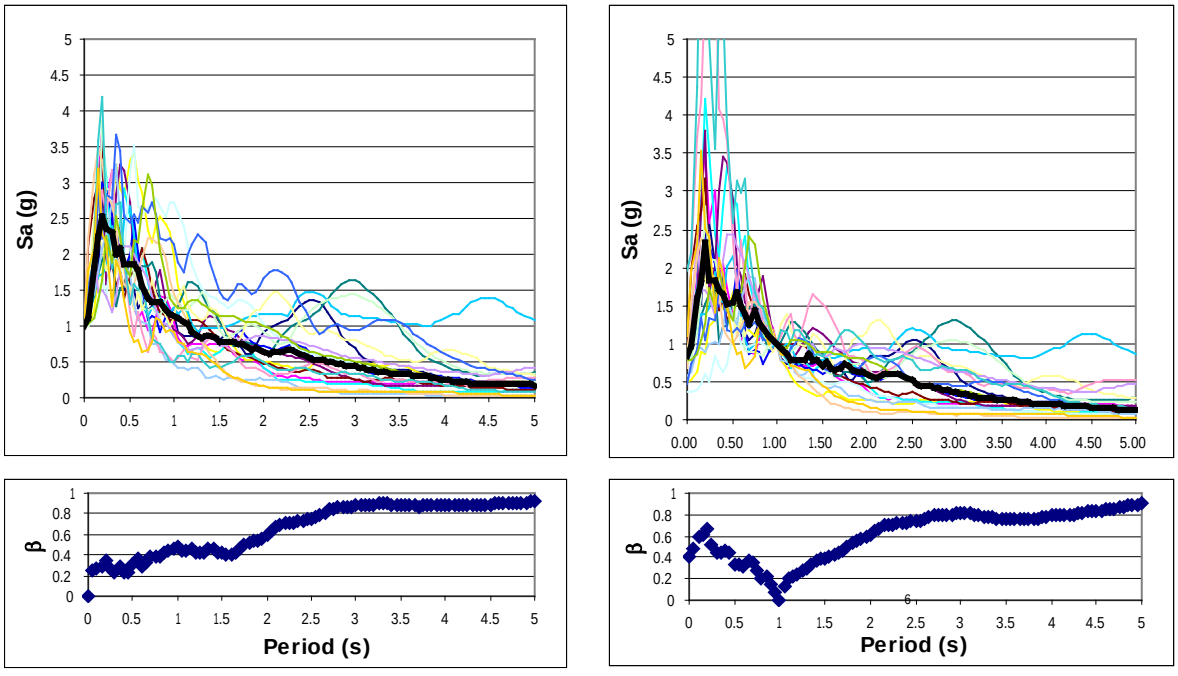

(a) (b)

Fig. 2 Spectral accelerations and lognormal standard deviations of the 20 ground motions scaled to a common IM of (a) PGA and (b) $S_a(T_n = 1\text{ s}, 5\%)$

[1] Website of PEER Strong Motion Database, http://peer.berkeley.edu/smcat/

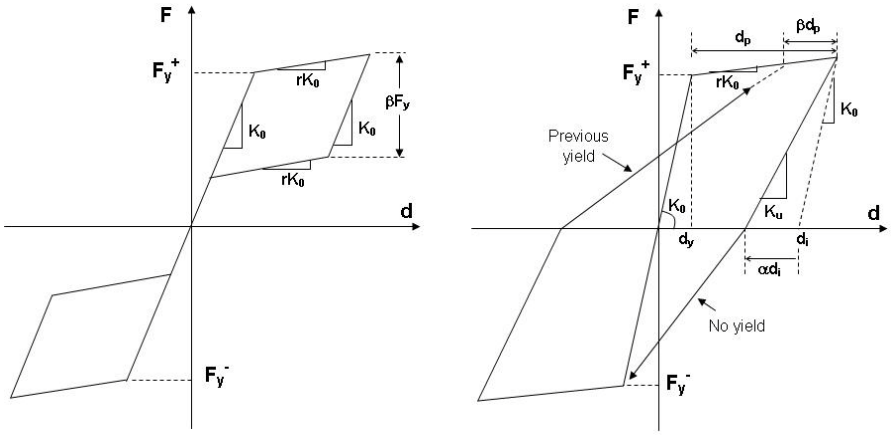

Fig. 3 Nonlinear models used for the dynamic analysis of walls

The maximum displacement response obtained from the time-history analysis for each intensity level (i.e., PGA) of an earthquake record is converted to drift (in %) by dividing it by the effective height of the wall. The so-obtained maximum drift and the IM of the earthquake record used in the analysis give the coordinates to locate one point in the PGA versus drift domain. Conducting several analyses with the same earthquake record scaled to different PGAs gives several points in the PGA versus drift plot, which can be joined to generate the IDA curve for that earthquake. Repeating the process with the 20 earthquake records in the compiled suite gives 20 IDA curves. In this study, these IDA curves are fitted to Ramberg-Osgood (R-O) equation (Ramberg and Osgood, 1943), and smoother IDA curves are redrawn using the fitted R-O parameters. Figure 4(a) presents the smoothened IDA curves along with their respective dispersions for the two different types of wall panels.

Due to variations in the characteristics of input ground motions, the maximum drift (i.e., EDP) of the wall generated by these records, even after scaling to the same IM, varies considerably. In order to incorporate this variation in responses, either a distribution needs to be assumed or a distribution-free numerical approach must be followed by carrying forward all the data points. This study adopts the former approach, i.e., a lognormal distribution is used to represent the variation in responses. In fact, previous studies (Cornell et al., 2003; Giovenale et al., 2004; Mander et al., 2007) have proved that the variation of IDA responses conforms closely to a lognormal distribution, which can be described by a median value $\tilde{x}$ and a lognormal coefficient of variation (β_D), also known as the dispersion factor. The median response $\tilde{x}$ can be obtained from the 50th percentile IDA curve, which is shown along with the 10th and 90th percentile IDA curves in Figure 4(b). These curves were generated by statistically analysing the variation of the 20 IDA curves shown in Figure 4(a).

2. Treatment of Epistemic Uncertainty and Aleotoric Variability

The variability in the IDA response is mainly due to the record-to-record randomness of the input motion (i.e., aleotoric uncertainty). This is because the computational modeling is conducted using crisp input data. However, the structural resistance both in terms of strength and displacement capacities is also inherently variable. To encompass the randomness of seismic demand along with the inherent randomness of the structural capacity and the uncertainty due to the inexactness of the computational modeling, it is necessary to use an integrated approach as suggested by Kennedy et al. (1980). The composite value of the lognormal coefficient of variation (i.e., dispersion factor) can be expressed as

$$\beta_{C/D} = \sqrt{\beta_C^2 + \beta_D^2 + \beta_U^2} \tag{2}$$

in which β_C is coefficient of variation for the capacity. This arises as a result of the randomness of the material properties that affect strength. In the case of precast wall panels, this is due to the randomness in the yield strength and is assumed to be equal to 0.2 for this study. Further, β_D in Equation (2) represents coefficient of variation for the seismic demand, which arises from record-to-record randomness in the earthquake ground motion suite. Also, β_U represents lognormal dispersion parameter for modelling uncertainty. It is assumed to be 0.25 in this study. The values of β_C and β_U assumed here are loosely

based on the FEMA-350 recommendations for the steel moment-resisting frames (FEMA, 2000), as the authors are unaware of any other authentic quantification of β_C and β_U for the RC walls.

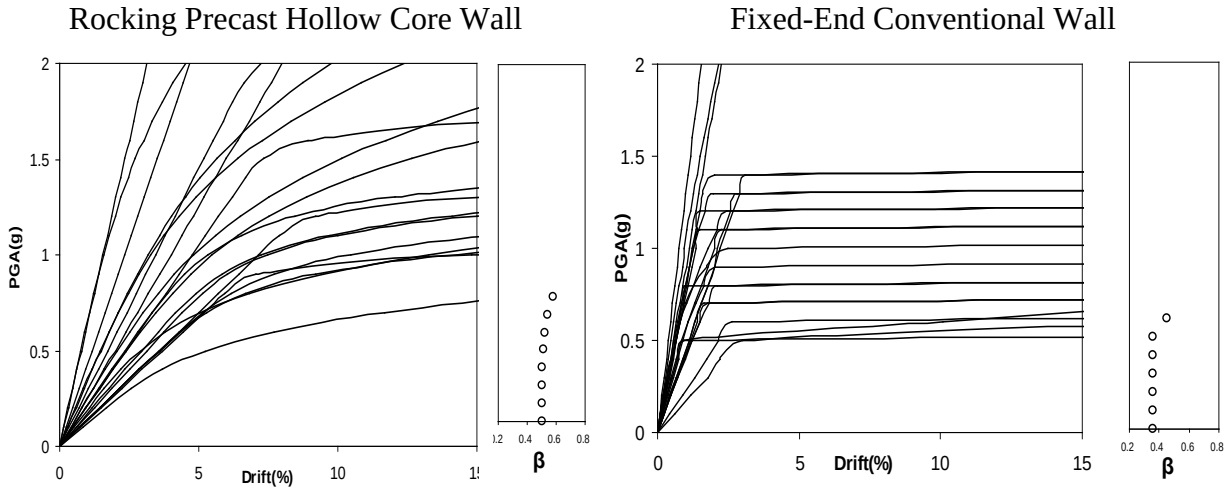

(a) IDA curves for the 20 records fitted to Ramberg-Osgood equation

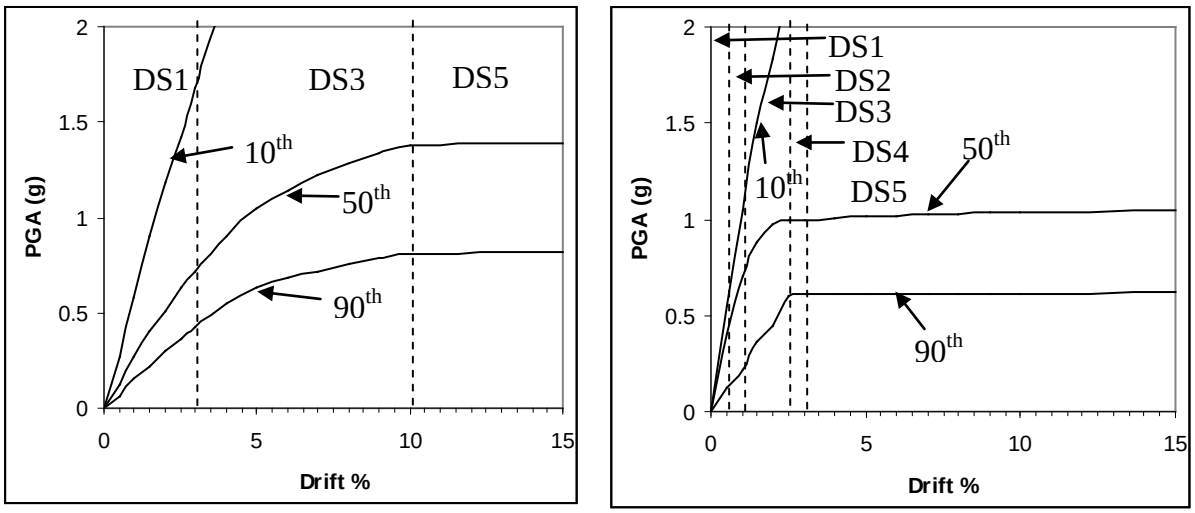

(b) Fitted IDA curves for different percentile response demands, with damage states indicated

Fig. 4 Performing IDA procedures and fitted IDA

EDP VERSUS DM RELATIONSHIP: THE DAMAGE MODEL

A common form of damage classification is to use a numerical indicator format as adopted by HAZUS (NIBS, 1999). As given in the first two columns of Table 2, numbers from 1 to 5 that refer to increasing level of damage are used. It may be noted that the first two columns of Table 2 give only the quantitative definition of damage states. However, in order to use Equation (1), we need EDPs corresponding to the different damage states. For this purpose, the experimental results of DAD and ductile wall panels tested by Hamid (2006) and Holden (2001) are used to define the drift limit states for different levels of damage.

1. Experimental Investigations on Ductile and DAD Walls

In New Zealand, many experimental investigations have been carried out to investigate seismic behaviour of monolithic ductile walls and precast DAD walls. Holden et al. (2003) pointed out the disadvantages of monolithic cast-in-situ walls, or precast concrete walls designed to behave as "if monolithic". Significant damage involving large residual lateral displacements and wide residual cracks is expected to occur with such systems, resulting in a considerable cost to the building owner. With an

intention of improving the seismic performance, precast prestressed concrete walls designed according to the DAD philosophy were used by Holden et al. (2003) in their experimental investigation. Two geometrically identical half-scale precast cantilever wall units were constructed and tested under quasi-static reversed cyclic lateral loading. One unit was a code-compliant conventionally reinforced concrete specimen, designed to emulate the behaviour of a ductile cast-in-situ wall. The other unit was a part of a precast partially prestressed system that incorporated post-tensioned unbonded carbon fiber tendons and steel-fibre reinforced concrete. Hysteretic energy dissipation devices were provided in the second unit in the form of low-yield-strength tapered longitudinal reinforcement bars, acting as a fuse connection between the wall panel and the foundation beam. The rocking wall had a steel plate at the bottom and diagonal reinforcing bars across up to one-third of the height of the wall. Using the strut-tie approach, the lateral forces were transferred to the unbonded post-tensioning carbon fibre, to the wall, and finally to the foundation beam. Dramix steel fibre was added to the concrete mix to control cracking by increasing the tensile strength of the concrete.

Table 2: Classification of Damage States, Drift Limits, Range of Loss Ratios and Assumed Loss Ratios for the Two Wall Systems

Damage State	Damage Description	Precast (DAD) Walls			Fixed-End Ductile Walls		
		Drift Limit	Loss Ratio		Drift Limit	Loss Ratio	
			Range	Assumed		Range	Assumed
1	No	-	-	-	-	-	-
2	Minor	-	-	-	0.5	0.05–0.15	0.1
3	Moderate / Repairable	3.0	Small	0.01	1.0	0.2–0.4	0.3
4	Severe / Irreparable	-	-	-	2.5	1.0–1.2	1.0
5	Collapse	10.0	1	1.0	3.0	1	1

The conventionally reinforced specimen (Unit 1) showed progressive damage starting with compressive spalling of the cover concrete at 2% drift and then buckling of the longitudinal bars at 2.5% drift. Finally, the outermost longitudinal bar fractured at 3% drift. The DAD rocking specimen (Unit 2) performed very well up to 6.2% drift without any strength degradation. Unit 2 performed significantly better than Unit 1 under seismic loading in spite of not satisfying the code requirements for transverse reinforcement and longitudinal steel as used in the standard ductile detailing practice. The drift ratios corresponding to different damage states for the ductile wall panel are decided based on the aforementioned experiment of Holden et al. (2003).

On the other hand, the EDP-DM relationship for the DAD wall is established from the results of recent rocking wall tests (Hamid, 2006). Two geometrically similar precast hollow-core walls were tested under reversed cyclic quasi-static loading. Both walls were designed to carry gravity loads and to resist lateral loads by rocking on their foundations. The specimens were detailed with steel-armouring at their base-to-foundation interfaces to provide a measure of damage protection. Results of these walls were similar to the results of the DAD wall test performed by Holden et al. (2003).

In this test series, the seismic performance of a super-assemblage of precast concrete hollow-core wall units, which is commonly used in a sidewall of a single-storey warehouse type building, was also investigated (Hamid, 2006). As shown in Figure 5(a), the super-assemblage had six precast wall panels, out of which the two extreme units were tied to the foundation via unbonded vertical prestress designed with the DAD philosophy, and the other four units were primarily acting as non-structural cladding. Figure 5(b) shows the overall performance of the multi-panel wall tested up to ±4.0% drift. It may be noted that there is a small residual deformation in the experimental loops. This is unintended and is accepted by the experimenter (Hamid, 2006) as an issue of concern because this is against the fundamental DAD objective of recentering. Moreover, buckling of the energy dissipater (mild steel) bars during the larger drift cycles led to a small reduction in strength and stiffness (i.e., softening). As the softening and residual displacement were not modelled in the “flag-shaped” loop used in the analyses (see Figure 3), the experimental loops (see Figure 5(b)) did not match perfectly with the predicted hysteresis. It may be noted that if an extrusion damper had been used instead of the mild steel bar, this buckling related softening would have not existed. In fact, rocking systems complying more strictly with the DAD

philosophy do not show any major softening because the core of the resistance in such structures comes from the prestressing tendon, which typically has strain hardening rather than softening in the post-yield range. Overall, it was observed that the super-assemblage of the multi-panel wall performed well up to 3.0% drift. Although there was no major structural damage to the wall, some damage was evident in the silicon sealant joining the two DAD wall panels with the other non-structural panels after 3% drift. As it is not difficult to reseal the inter-unit connection and to replace the dissipaters, if needed, this state of damage is categorised as moderate and repairable.

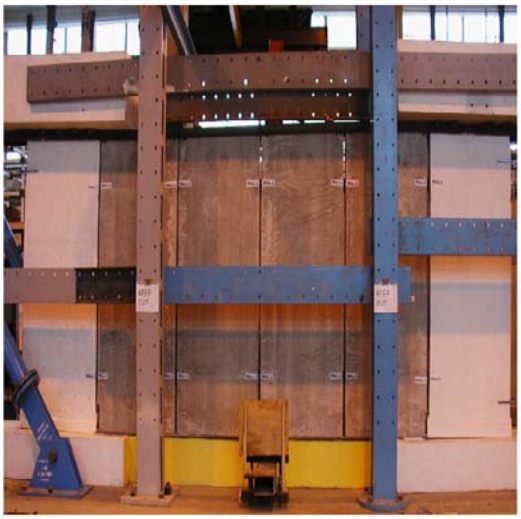

(a)

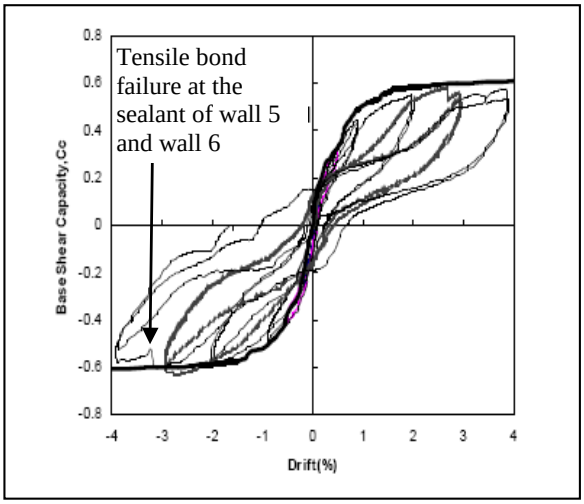

(b)

Fig. 5 (a) Multi-panel super-assemblage specimen representing part of the precast concrete hollow-core wall system, and (b) the overall hysteretic performance up to 4% drift of the specimen, for warehouse buildings tested by Hamid (2006)

2. Classification of Observed Building Damage

Based on the aforementioned experimental observations, the drift limits corresponding to the boundaries of different damage states are established for the two wall systems as summarised in Table 2. As the damage state classification given in Table 2 was proposed for the conventional ductile system, it is readily applicable for the ductile walls but needs to be amended for the DAD walls. In order to retain the same format, the damage of DAD walls is also classified here in three categories: DS1 for no damage; DS3 for reparable (though minor) damage corresponding to the loosening of prestressing tendons and spalling of sealant between the structural DAD wall panels and the non-structural panels; and DS5 corresponding to the final collapse. As the DAD walls are conceived in terms of damage avoidance, DS2 (slight damage) and DS4 (irreparable damage) are deemed not to exist.

The first damage state (i.e., DS1), being for no damage, will obviously start at zero drift. The third damage state (i.e., DS3) of the DAD walls is defined on the basis of minor non-structural distress that will commence with the failure of sealant used to fill the vertical joints between the wall panels in a building, as observed in the tests at around 3.0% drift. Obviously, the last damage state (i.e., DS5) is the state of complete collapse, which for the DAD walls, corresponds to the drift where toppling or global instability occurs. In the previously described tests, the DAD walls did not collapse within the test regime, i.e., up to a drift limit of 6.2%. Therefore, the drift limit corresponding to DS5 was decided to be lesser of the drift corresponding to the ultimate (rupturing) strain of the prestressing tendon and the drift corresponding to the toppling of the wall. Based on the principles of rigid-body kinematics, this drift was estimated to be 10%. However, as would be apparent in the subsequent steps later, the results of seismic financial risk analysis remain unaffected by any change in the drift values in the range of around 10%. It is to be noted that the 10% drift (which is apparently high) is used herein to represent the collapse of the rocking wall only and should not be mistaken as the deformability of a building having such walls. When the subject of investigation is a complex structure where the wall is only a component, the collapse of the structure will have to be correlated to the lowest drift corresponding to the collapse of all critical structural components, not only that of the wall.

During the test of the fixed-end monolithic wall (Holden, 2001), the first noticeable damage (i.e., DS2) occurred at the yielding of external longitudinal reinforcement at 0.5% drift. At this stage, there were also some minor cracks in both sides of the wall. In fact, these flexural crack had emerged much earlier in the test, but were not taken seriously until the yielding of bars widened these cracks. In the experiment, the wall suffered a repairable damage (i.e., DS3) when the drift was 1%. At this stage, the wall had large residual cracks (exceeding 2 mm in width) and 0.4% residual drift. At 2.5% drift, the outermost longitudinal reinforcing bars buckled and began to fracture. Significant residual drift of about 1.5% remained at this damage state. This damage is classified here as irreparable damage corresponding to DS4. The experimental results showed that the wall started to lose its strength and subsequently lost its stability when subjected to further repeated cycles at this drift. As all the longitudinal reinforcing bars buckled and fractured with severe damage occurring in concrete at drift exceeding 3.0%, 3.0% is used as the drift limit corresponding to the onset of DS5.

The different damage states for the two wall systems are also shown, together with the IDA curves, in Figure 4(b). It is interesting to note in Figure 4(b) that there is no change in the PGA values above the 2.5% drift level for the ductile wall system. Due to this, IM and the corresponding annual probabilities will coincide for DS4 and DS5 in the case of ductile walls. As will be seen later, this will result in the disappearance (i.e., no contribution) of the DS4 range in the fragility curves and subsequent EAL calculation procedure.

ASSESSMENT OF HAZARD SURVIVAL PROBABILITY

1. DM versus IM: Generation of Fragility Curves

The points of intersection of the vertical dashed lines representing the boundaries between different damage states and the 50th percentile IDA curve in Figure 4(b) give the median IMs corresponding to the onset of these damage states. Using these median values and the composite lognormal coefficient of variation, $\beta_{C/D}$, calculated earlier using Equation (2), the cumulative probability of exceeding each of the damage states for a given IM can be calculated. This can be graphically shown in the form of fragility curves, which are shown in Figure 6(a) for the two wall systems analysed in this study. Two vertical lines are drawn at 0.4*g* and 0.72*g* to represent respectively the design basis earthquake (DBE) and the maximum considered earthquake (MCE) at Wellington, following the seismic hazard map reported in the New Zealand loading standard NZS 1170.5 (NZS, 2004). The intersection of each of these vertical lines with the fragility curves gives the probabilities of damage exceeding different damage states for the corresponding seismic hazard (i.e., DBE or MCE).

Figure 6(a) shows that 50% DAD walls would be expected to sustain no damage (under the damage state DS1) during an MCE. Among the rest, 40% would be expected to require minor inexpensive repairs. Nature of these repairs may be like tightening prestressing tendons, replacing mechanical energy dissipaters (if provided), and replacing peeled off sealant. The remaining 10% DAD walls would be expected to topple down (under the damage state DS5) requiring demolition of the building after an MCE. Similarly it is also evident from Figure 6(a) that only 2% or less of the DAD walls may be expected to topple under a DBE, and another 10% would be requiring small repairs as mentioned earlier. The remaining 88% DAD walls will have no damage under a DBE.

Looking at the fragility curves for the ductile walls in Figure 6(a), it can be noticed that only 12% of such walls are expected to remain undamaged and another 36% are likely to experience slight damage during an MCE. Severe or irreparable damage would be expected in 52% ductile walls, among which 25% are likely to collapse. Under a DBE, 13% ductile walls are expected to undergo severe damage, among which 3% are expected to collapse. Only 50% of the ductile walls are expected to have slight or no damage during a DBE.

2. IM versus f_a : Earthquake Recurrence Relationship

It may be noted that the fragility curves shown in Figure 6(a) are plots of the conditional probability of a damage measure for a given IM (i.e., *P*[DM|IM], which is the product of *P*[DM|EDP] and *P*[EDP|IM]) against IM (i.e., PGA in this study). In order to use these curves as a part of Equation (1), the

horizontal axis needs to be annual probability (f_a) rather than the hazard intensity. Hence, it is necessary to define a relationship between the annual probability of earthquakes and their intensity.

Based on historical earthquake data, relationship of the peak ground acceleration (PGA) of earthquake ground motions (denoted by a_g) with their annual probability of occurrence (f_a) has been established, as shown in Figure 6(b), and is given by

$$a_g = \frac{a_g^{\mathrm{DBE}}}{(475 f_a)^q} \tag{3}$$

where a_g^{DBE} is the PGA corresponding to the DBE (with 10% probability of occurrence in 50 years), and q is an empirical constant found to be equal to 0.33 for seismic hazard in New Zealand (NZS, 2004).

3. DM versus f_a : Hazard Survival Curves

Fragility curves of Figure 6(a) can now be re-plotted by changing the horizontal axis from IM to f_a and by using the earthquake recurrence relationship of Equation (3). Such curves are called "hazard-survival curves" in this paper, and they show the probability of damage being within a limit state when an earthquake of a given annual probability strikes. Figure 6(c) compares the hazard survival curves for the DAD and ductile wall systems. Two vertical lines representing the annual probabilities of DBE (f_a ~ 0.002) and MCE (f_a ~ 0.0004) are also shown in the plots for reference. The intersections of any vertical line through a value of f_a with the hazard survival curves give the probabilities of these damage states not being exceeded during the earthquakes of that annual probability of occurrence. These hazard curves can also be used to estimate the confidence intervals, i.e., the confidence of being inside the range of different damage states. For example, Figure 6(c) indicates that if an MCE strikes, the probability of DS1 not being exceeded in DAD walls is about 48%, and there is only 10% probability of DS3 being exceeded (i.e., entering into the collapse state DS5). This can also be interpreted to imply that during an MCE, there is a 48% chance that a precast DAD wall will not be damaged (under the damage state DS1), about 42% chance that repairing due to the loosening of tendons and peeling off of sealant will be needed (under the damage state DS3), and 10% chance that the wall will collapse (under the damage state DS5). In other words, out of 100 DAD walls, 48 are likely to remain undamaged during an MCE, 42 are likely to undergo slight damage, and the remaining 10 are likely to collapse due to toppling. Similar interpretation can be made for the ductile walls based on Figure 6(c).

FINANCIAL IMPLICATIONS OF EARTHQUAKES

1. DM versus L_R : Loss Model

To quantify financial loss, a loss model must be established to relate damage measure (DM) to a dollar value. In this study, the financial implication of each damage state is represented by a "loss ratio" (L_R), which is the ratio of the repair/retrofit cost necessary to completely restore the functionality of the structure to the replacement cost. To facilitate comparison between the loss ratios, original costs of these two walls must also be known. In terms of materials, the area of the hollow core section of the DAD wall is half of that of the ductile wall (see Figure 1). Moreover, no reinforcing bars and stirrups are needed in the DAD walls but prestressing strands are required instead. Additionally, the external energy dissipaters are also required in the DAD walls. Hence, the material costs are comparable in these two schemes. As DAD walls are precast, the construction and overhead costs are less for the DAD walls than for the ductile walls. Overall, the costs of these two wall systems are not much different, and the loss ratios can hence be compared directly without considering their absolute costs.

Table 2 lists the likely ranges and the assumed values of these loss ratios for different damage states for the two wall systems. For both wall systems, as DS1 refers to "no damage" state, no repair is necessary and the loss ratio for DS1 is therefore zero. As explained earlier, DS3 for the DAD walls constitutes damages that need minor non-structural repairs such as retightening of prestressing tendons, and replacing energy dissipaters and sealant. Therefore very little expense is expected and the loss ratio

for DS3 is likely to remain very small, and a representative value L_R = 0.01 is assumed in this study. For the DAD walls, as DS5 refers to toppling of the wall resulting in a collapse of building (thus needing a complete replacement), the value of loss ratio for DS5 is 1. It is already mentioned that Damage States 2 and 4 do not exist for the DAD walls; hence no loss ratios are assigned to DS2 and DS4.

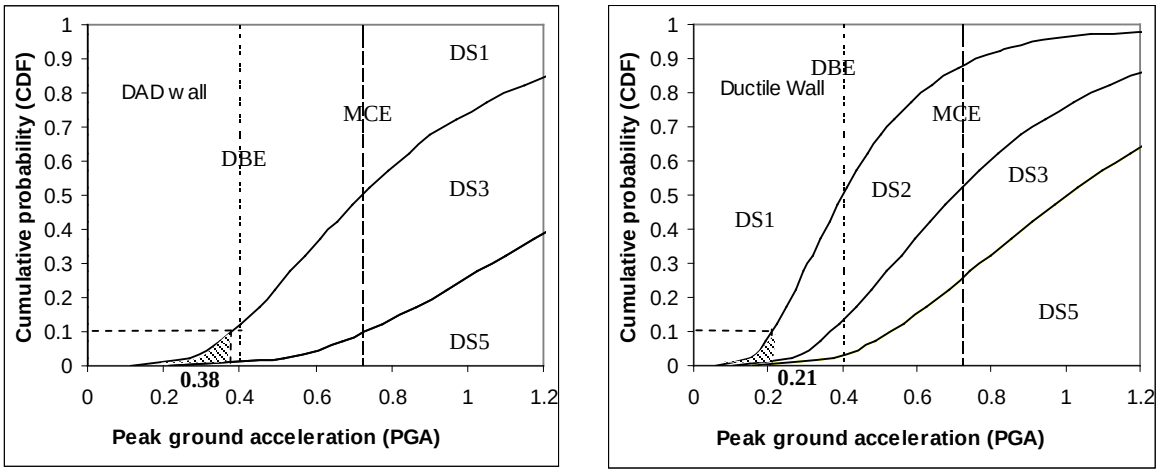

(a)

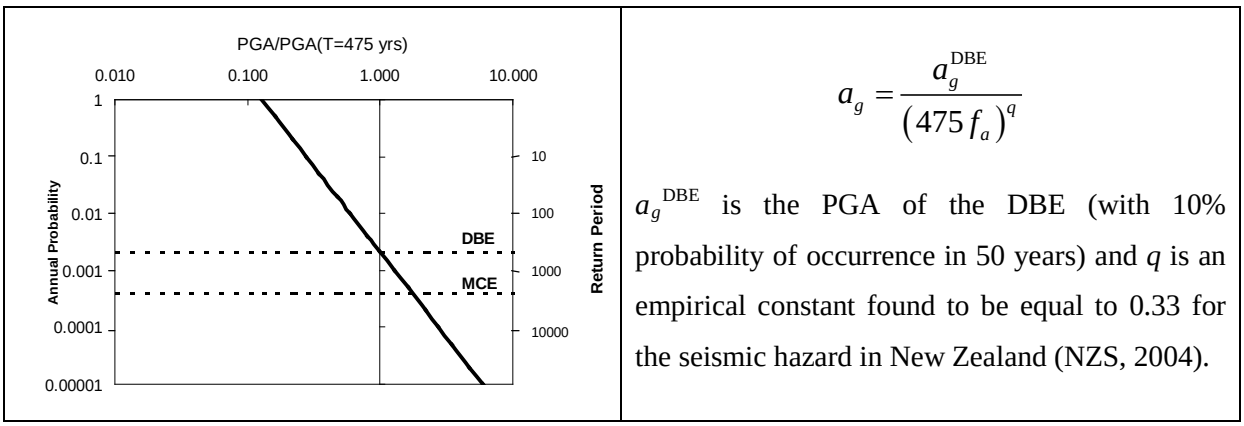

$$a_g = \frac{a_g^{\mathrm{DBE}}}{(475 f_a)^q}$$

a_g^{DBE} is the PGA of the DBE (with 10% probability of occurrence in 50 years) and q is an empirical constant found to be equal to 0.33 for the seismic hazard in New Zealand (NZS, 2004).

(b)

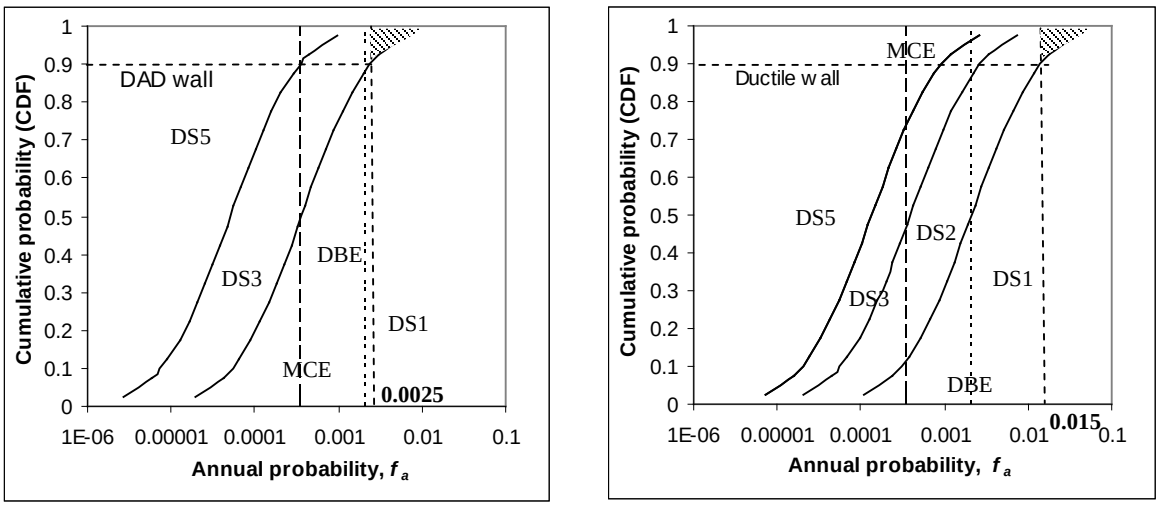

(c)

Fig. 6 (a) Fragility curves for the wall systems; (b) Hazard recurrence relation (between PGA (a_g) and annual probability (f_a)); (c) Hazard-survival curves for the two wall systems

For the ductile walls, the loss ratio L_R for DS2 is likely to fall between 0.05 and 0.15 to account for minor repairs to fix the slight but tolerable damage, and the median value of 0.1 is assumed for DS2. Similarly the loss ratio for DS3 may vary from 0.2 to 0.4 to repair the incurred moderate damage, or more likely to retrofit the damaged wall to completely restore the functionality, and a representative median value of 0.3 is adopted in the present analysis. The "irreparable damage" under DS4 demands complete replacement, as repair may be uneconomical; hence the loss ratio of 1 is used here. Similarly for DS5, which is a case of complete failure/collapse, the value of loss ratio is 1. The loss ratio value for DS1 (i.e., no damage) is undoubtedly zero as the definition suggests. Similarly, for DS5 (i.e., collapse) and DS4 (i.e., irreparable damage), the loss ratio has to be 1 or slightly higher if demolition cost is taken into account. Hence, the room for uncertainty exists only in the definition of DS3 for the DAD walls and DS2 and DS3 for the ductile walls. As studies scrutinizing the repair costs of DAD and ductile walls and their variation with the extent of damage are unknown to the authors, representative estimates based on engineering judgment are made for the loss ratios corresponding to these intermediate damage states.

2. L_R versus f_a: Probable Loss in an Earthquake

Using the assigned loss ratios, the contributions of different damage states to the financial loss can be estimated. The probable financial loss (as a fraction of the total replacement cost) due to a given damage state, when earthquakes with a given annual probability strike, can be calculated as the product of the probability of being in that damage state during the earthquakes of that annual probability (as obtainable from Figure 6(c)) and the assumed loss ratio for the damage state (as obtainable from Table 2). The contributions of different damage states to the total probable loss during the earthquakes of different annual probabilities are shown graphically in the form of bar charts in Figure 7(a). As expected, DS1 does not incur any financial loss, as it does not need any repair. Similarly, the financial loss incurred by the earthquakes of 0.1 or higher annual probability is also nil, as such frequent events do not incur any damage requiring repair, retrofit or replacement (i.e., under the DS2 or higher damage category). As the confidence intervals of higher damage states are multiplied by a higher loss ratio, the higher damage states contribute more to the probable loss, although the likelihood of the earthquake-induced damage falling in these more severe categories is not high.

Figure 7(b) compares the economic hazard curves, which are the plots showing the total probable loss ratio (i.e., summation of the contributions of all damage states) against the annual probability for the two wall systems. These curves give information on what would be the financial loss if an earthquake of a given annual probability strikes once. As expected, larger and more infrequent the earthquake is, greater will be the financial loss. Conversely, for frequent but low-intensity events, the single-event loss is small. Two vertical lines corresponding to DBE and MCE are also shown in the plots. It is evident from Figure 7(b) that ductile walls are likely to lose about 10% and 36% of their value due to the damage incurred by a DBE (i.e., a 10% in 50 years event) and an MCE (i.e., a 2% in 50 years event), respectively. A loss of 2% is possible even with the earthquakes of 0.01 annual probability (i.e., with a return period of 100 years). Similarly, about 19% loss is possible during an earthquake of 1000 years return period or with the annual probability $f_a \approx 0.001$. On the other hand, DAD walls will sustain a DBE almost without any damage (with the loss less than 1%). A total loss of 2% is expected in the DAD walls due to an earthquake with 0.001 annual probability (or 1000 years return period). There is only 10% chance that a DAD wall may collapse during an MCE, as opposed to 36% for a ductile wall.

SEISMIC ANNUAL FINANCIAL RISK

1. Calculation of Expected Annual Loss (EAL)

The total expected annual loss can be calculated by using Equation (1) by integrating the loss ratio (L_R) over all possible seismic hazards, i.e., annual frequencies between 0 and 1. This general equation in continuous form can be expressed as

$$\text{EAL} = \int_0^1 L_R \mathrm{d}f_a \tag{4}$$

From this equation, it is obvious that EAL is analogous to the total area under the economic hazard curve (in Figure 7(b)). Thus the calculated values of EAL are 0.117% and 0.017% of the total value (i.e., the replacement cost) for the ductile walls and DAD walls, respectively. Figure 7(c) compares the possible annual financial losses of the two types of walls due to the earthquakes of annual probabilities within different ranges. These probable losses are calculated as the area subtended by the economic hazard curves (see Figure 7(b)) between two points on the *x*-axis. It may be noted that the annual probability is plotted on the logarithmic scale in Figure 7(b), and that the absolute value of the interval between any two points on the *x*-axis decreases by an order of ten towards the left. Accordingly, the absolute value of the area covered also decreases rapidly in that direction (i.e., in the direction of decreasing probability) in spite of an increasing trend of total loss ratio in that direction.

As can be observed from Figure 7(c), the EAL of a DAD wall ($171/$1 million value) is approximately 15% of that of a ductile wall ($1170/$1 million value). For the ductile walls, 26% of this value (i.e., $308) corresponds to the risk posed by the frequent but modest size earthquakes with an annual frequency in the range between 0.01 and 0.1 (i.e., with return periods between 10 and 100 years). On the other hand, no contribution comes from these frequent but modest size earthquakes to the annual financial loss expected for the DAD walls.

This model is likely to overestimate the EAL by including the contributions of frequent events with very low return periods (i.e., with very high annual frequency f_a values) although they might not necessarily cause any damage. This error can be compensated by restricting the upper limit of integration in Equation (4) to a threshold frequency that corresponds to a high confidence of not inducing any damage. This threshold is decided in this paper by locating the IM and the corresponding f_a for which the probability of no damage (i.e., of remaining in DS1) is 90%. The so obtained threshold IM and f_a for the ductile and DAD walls are shown by the dashed lines in Figures 6(a) and 5(c). For example, to have at least 10% chance of inducing any damage (i.e., under DS2) to the ductile walls, earthquakes with the PGAs of at least 0.21*g* (i.e., with the annual probability of 0.015) are required. Similarly the decided approximate values for the threshold IM and f_a for the DAD walls are 0.38*g* and 0.0025, respectively. The EALs of the ductile and DAD walls reduce, respectively, to $941 and $157 per $1 million of the asset value if these thresholds are applied in the integration. Thus, the reduction of EAL by ignoring the contributions of the earthquakes below the threshold IM (i.e., above the threshold frequency) for the DAD and ductile walls is 8% and 20%, respectively.

2. Implications for Owners and Insurers

Vertical ordinate of an economic hazard curve shown in Figure 7(b) gives the total probable loss due to the scenario earthquake of a given annual probability. Hence, these curves also represent the financial consequences of different earthquakes to owners of industrial warehouse type buildings with the two different wall systems. Evidently, earthquakes that are smaller and more frequent than the DBE cause negligible loss to the owners of buildings with DAD walls and a small loss (which is less than 9%) to the owners of warehouse buildings with fixed-end ductile walls. Consequently, owners may be prepared to bear the consequences of these frequent earthquakes by themselves. For example, in the worst case, the owners of fixed-end ductile wall buildings may need to spend a small sum (which is less than 2% of the building value) to repair the damage (if any) incurred if and when moderate earthquakes with return periods of 100 years or less ($f_a \geq 0.01$) strike. On the other hand, the consequences of rarer but stronger earthquakes may be disastrous, often incurring 50% or more loss, thereby rendering the repair uneconomical, and necessitating replacement. Building owners would obviously be more inclined to pass this risk to insurers.

It may be noted that the total risk encompasses consequences of all probable hazards. In other words, the integration of the economic hazard curve (as in Figure 7(b)) represents the total seismic financial risk. As EAL is the area subtended by the economic hazard curve, it represents the likely economic loss in a year due to all probable earthquakes and is directly related to an annual insurance premium excluding the overhead and profit components. Looking at the contributions of earthquakes of different frequency ranges to the EAL in Figure 7(c), it is apparent that the more frequent and smaller earthquakes have a large contribution to the annual financial risk, whereas the large earthquakes contribute significantly less to the annual financial risk due mainly to their very small probability of occurrence (or long return

period). Nevertheless, most insurance and re-insurance policies are targeted to cover these rarer and bigger hazards because of their disastrous consequences. In contrast, the smaller and more frequent earthquakes may cause a small loss to the individual owners but a significant collective risk to the insurers. From the insurance point-of-view, the loss due to these smaller and more frequent events should ideally be born by the owner. This can be achieved by setting an appropriate deductible to the insurance policy. Obviously, a higher deductible would reduce the insurance premium.

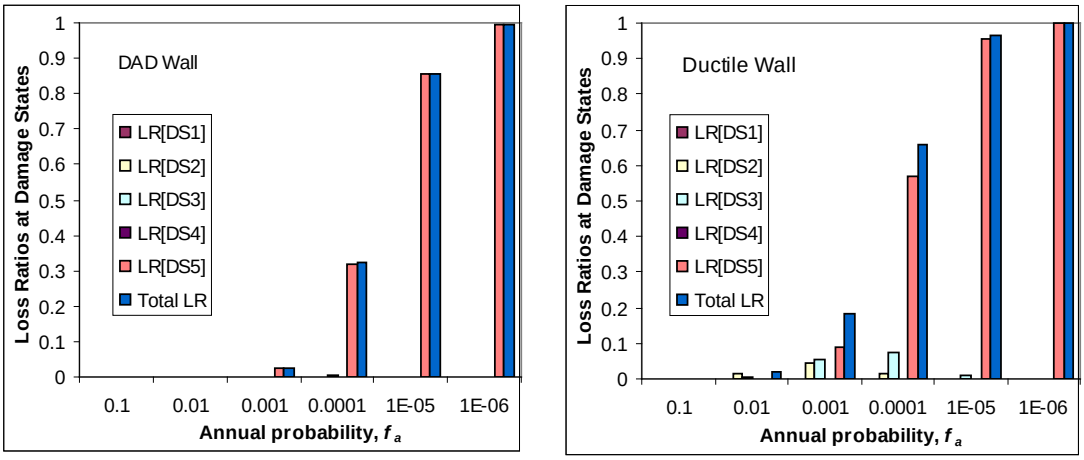

(a)

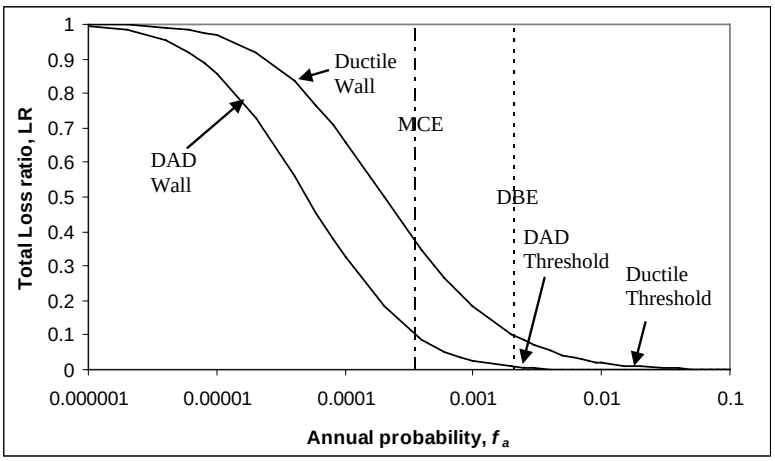

(b)

Wall System	EAL ($ / $1 million)	
	No Threshold	With Threshold
DAD	171	157
Ductile	1170	941

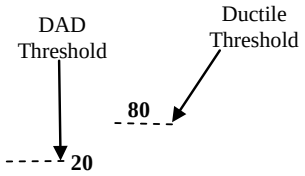

(c)

Fig. 7 (a) Loss ratios inflicted by different damage states to the two wall systems; (b) Economic hazard curves; (c) Annual financial risk due to the earthquakes of different probabilities

CONCLUSIONS AND RECOMMENDATIONS

The structural performance, fragility, hazard-survival probability, and the associated financial risk of monolithic ductile walls and precast DAD walls have been compared. Results of experimental investigations on the seismic performance of fixed-end ductile walls and rocking precast walls designed with the DAD philosophy have been extended to assess the seismic financial risk. Expected annual loss (EAL) has been calculated by using a generalised probabilistic financial risk assessment methodology for the two walls. It has been concluded that ductile walls are inferior to DAD walls, both in terms of structural performance and financial risk. A loss of about 36% has been estimated for the monolithic ductile walls during an MCE (i.e., a 2% in 50 years event) and 10% during a DBE (i.e., a 10% in 50 years event). On the other hand, precast DAD walls will have no loss during a DBE and less than 10% loss during an MCE. The estimated EAL of the DAD walls is only 15% of the EAL of the ductile walls.

The findings of this study have also led to a conclusion that very large earthquakes contribute very little to the total annual financial risk due to their very low probability of occurrence, although structures are likely to partially or completely collapse if the rare earthquakes of such magnitudes strike, thereby creating a scary situation for the individual owners and insurers. On the other hand, smaller earthquakes may cause only minor-to-moderate damage and repairing it may not cause significant financial problem to the owners; however, these small-to-moderate earthquakes pose a big collective risk to the insurers as they are likely to strike more often. Thus, the not-so-high risk posed by the frequent and moderate earthquakes may be borne by the owners by setting a deductible in low-premium insurance policies, which are mainly aimed to cover the disastrous consequences of rare and strong earthquakes. Calculations have shown that earthquakes with return periods between 10 and 100 years would contribute approximately 26% to the annual financial risk in the case of monolithic ductile walls. These frequent earthquakes, however, will cause no damage, and hence no financial loss, to the precast DAD walls. This indicates that probable loss due to the damage of structural and non-structural walls can be mitigated greatly by adopting the damage avoidance design principles.

Although this study has given interesting and useful qualitative information on the relative seismic performance and financial implications of the two wall systems, there is room for improvement that will lead to more reliable and more useful quantitative outcomes. As this study had aimed to explain the application of the proposed financial risk assessment procedure, the target structure was intentionally chosen to be a simple component (i.e., wall) rather than a more complex structural system (such as a building) consisting of a number of different components. It is for this reason that the losses arising from structural and non-structural damages of other components, acceleration-sensitive content damage, downtime, and death became irrelevant in this study. Definitely, more useful information would be obtained if the subject of the seismic risk assessment procedure were a building where all sources of losses are accounted for. Although uncertainties in capacity and demand were incorporated in the form of corresponding lognormal coefficients of variations, the inevitable uncertainties in the experiment-based damage model and the engineering judgment-based loss model have not been accounted for. The best-estimate values assigned to the drift ratios and loss ratios for different damage states are also somewhat subjective. Hence, future studies should try to establish more robust damage and loss models, and investigate their uncertainties, so that those could be accounted for while estimating financial risk.

ACKNOWLEDGEMENTS

The first author wishes to thank National Programme on Earthquake Engineering Education (NPEEE) of Ministry of Human Resources & Development, Government of India for awarding him a fellowship for conducting this research. He also expresses his gratitude to S.G.S. Institute of Technology and Science, Indore, India and to University of Canterbury, Christchurch, New Zealand for providing him all the necessary facilities.

REFERENCES

1. Ajrab, J.J., Pekcan, G. and Mander, J.B. (2004). “Rocking Wall-Frame Structures with Supplemental Tendon Systems”, Journal of Structural Engineering, ASCE, Vol. 130, No. 6, pp. 895–903.

2. Arnold, D.M. (2004). "Development and Experimental Testing of a Seismic Damage Avoidance Designed Beam to Column Connection Utilising Draped Unbonded Post-Tensioning", M.E. Thesis, Department of Civil Engineering, University of Canterbury, Christchurch, New Zealand.
3. Bora, C., Oliva, M.G., Nakaki, S.D. and Becker, R. (2007). "Development of a Precast Concrete Shear-Wall System Requiring Special Code Acceptance", PCI Journal, Vol. 52, No. 1, pp. 122–135.
4. Carr, A.J. (2003). "RUAUMOKO: Inelastic Dynamic Analysis Program", User's Manual, Department of Civil Engineering, University of Canterbury, Christchurch, New Zealand.
5. Cornell, C.A., Jalayer, F., Hamburger, R.O. and Foutch, D.A. (2002). "Probabilistic Basis for 2000 SAC Federal Emergency Management Agency Steel Moment Frame Guidelines", Journal of Structural Engineering, ASCE, Vol. 128, No. 4, pp. 526–533.
6. Dhakal, R.P. and Mander, J.B. (2006). "Financial Risk Assessment Methodology for Natural Hazards", Bulletin of the New Zealand Society for Earthquake Engineering, Vol. 39, No. 2, pp. 91–105.
7. FEMA (2000). "Recommended Seismic Design Criteria for New Steel Moment-Frame Buildings", Report FEMA-350, Federal Emergency Management Agency, Washington, DC, U.S.A.
8. Giovenale, P., Cornell, C.A. and Esteva, L. (2004). "Comparing the Adequacy of Alternative Ground Motion Intensity Measures for the Estimation of Structural Responses", Earthquake Engineering & Structural Dynamics, Vol. 33, No. 8, pp. 951–979.
9. Hamid, N.B.A. (2006). "Seismic Performance of Precast Hollow-Core Wall Panels under Bi-lateral Reverse Quasi-static Lateral Loading Simulated with Gravity Loading", Ph.D. Thesis, Department of Civil Engineering, University of Canterbury, Christchurch, New Zealand.
10. Holden, T.J. (2001). "A Comparison of the Seismic Performance of Precast Wall Construction: Emulation and Hybrid Approach", M.E. Thesis, Department of Civil Engineering, University of Canterbury, Christchurch, New Zealand.
11. Holden, T.J., Restrepo, J.I., Mander, J.B. (2003). "Seismic Performance of Precast Reinforced and Prestressed Concrete Walls", Journal of Structural Engineering, ASCE, Vol. 129, No. 3, pp. 286–296.
12. Kennedy, R.P., Cornell, C.A., Campbell, R.D., Kaplan, S. and Perla, H.F. (1980). "Probabilistic Seismic Safety Study of an Existing Nuclear Power Plant", Nuclear Engineering and Design, Vol. 59, No. 2, pp. 315–338.
13. Krawinkler, H. and Miranda, E. (2004). "Performance-Based Earthquake Engineering" in "Earthquake Engineering: From Engineering Seismology to Performance-Based Engineering (edited by Y. Bozorgnia and V.V. Bertero)", CRC Press, Boca Raton, U.S.A.
14. Kurama, Y.C. (2000). "Seismic Design of Unbonded Post-Tensioned Precast Concrete Walls with Supplemental Viscous Damping", ACI Structural Journal, Vol. 97, No. 4, pp. 648–658.
15. Kurama, Y.C. (2005). "Seismic Design of Partially Post-Tensioned Precast Concrete Walls", PCI Journal, Vol. 50, No. 4, pp. 100–125.
16. Kurama, Y., Sause, R., Pessiki, S. and Lu, L.W. (1999). "Lateral Load Behaviour and Seismic Design of Unbonded Post-Tensioned Precast Concrete Walls", ACI Structural Journal, Vol. 96, No. 4, pp. 622–632.
17. Kurama, Y., Sause, R., Pessiki, S. and Lu, L.W. (2002). "Seismic Response Evaluation of Unbonded Post-Tensioned Precast Nails", ACI Structural Journal, Vol. 99, No. 5, pp. 641–651.
18. Li, L. (2006). "Further Experiments on Damage Avoidance Design of Beam-to-Column Joints", M.E. Thesis, Department of Civil Engineering, University of Canterbury, Christchurch, New Zealand.
19. Mander, J.B. and Cheng, C.-T. (1997). "Seismic Resistance of Bridge Piers Based on Damage Avoidance Design", Technical Report NCEER-97-0014, State University of New York at Buffalo, Buffalo, U.S.A.
20. Mander, J.B., Dhakal, R.P., Mashiko, N. and Solberg, K.M. (2007). "Incremental Dynamic Analysis Applied to Seismic Financial Risk Assessment of Bridges", Engineering Structures, Vol. 29, No. 10, pp. 2662–2672.
21. Mashiko, N. (2006). "Comparative Performance of Ductile and Damage Protected Bridge Piers Subjected to Bi-directional Earthquake Attack", M.E. Thesis, Department of Civil Engineering, University of Canterbury, Christchurch, New Zealand.

22. Michael, D.N. (2003). “Seismic Damage Avoidance Design of Beam-Column Joints Using Unbonded Post-Tensioning: Theory, Experiments and Design Example”, M.E. Thesis, Department of Civil Engineering, University of Canterbury, Christchurch, New Zealand.
23. NIBS (1999). “Earthquake Loss Estimation Methodology HAZUS: Technical Manual”, Report prepared for the Federal Emergency Management Agency, National Institute of Building Sciences, Washington, DC, U.S.A.
24. NZS (2004). “NZS 1170.5:2004, Structural Design Actions, Part 5: Earthquake Actions—New Zealand”, Standards New Zealand, Wellington, New Zealand.
25. Perez, F.J., Pessiki, S. and Sause, R. (2004). “Seismic Design of Unbonded Post-Tensioned Precast Concrete Walls with Vertical Joint Connectors”, PCI Journal, Vol. 49, No. 1, pp. 58–79.
26. Ramberg, W. and Osgood, W.R. (1943). “Description of Stress-Strain Curves by Three Parameters”, Technical Note No. 902, National Advisory Committee for Aeronautics, Washington, DC, U.S.A.
27. Vamvatsikos, D. and Cornell, C.A. (2002). “Incremental Dynamic Analysis”, Earthquake Engineering & Structural Dynamics, Vol. 31, No. 3, pp. 491–514.
28. Vamvatsikos, D. and Cornell, C.A. (2004). “Applied Incremental Dynamic Analysis”, Earthquake Spectra, Vol. 20, No. 2, pp. 523–553.